Bub3 promotes Cdc20-dependent activation of the APC/C in *S. cerevisiae*

Yang Yang, Dai Tsuchiya, and Soni Lacefield

Department of Biology, Indiana University, Bloomington, IN 47405

The spindle checkpoint ensures accurate chromosome segregation by sending a signal from an unattached kinetochore to inhibit anaphase onset. Numerous studies have described the role of Bub3 in checkpoint activation, but less is known about its functions apart from the spindle checkpoint. In this paper, we demonstrate that Bub3 has an unexpected role promoting metaphase progression in budding yeast. Loss of Bub3 resulted in a metaphase delay that was not a consequence of aneuploidy or the activation of a checkpoint. Instead, *bub3Δ* cells had impaired binding of the anaphase-promoting complex/cyclosome (APC/C) with its activator Cdc20, and the delay could be rescued by Cdc20 overexpression. Kinetochore localization of Bub3 was required for normal mitotic progression, and Bub3 and Cdc20 colocalized at the kinetochore. Although Bub1 binds Bub3 at the kinetochore, *bub1Δ* cells did not have compromised APC/C and Cdc20 binding. The results demonstrate that Bub3 has a previously unknown function at the kinetochore in activating APC/C-Cdc20 for normal mitotic progression.

Introduction

Anaphase onset is regulated by the anaphase-promoting complex/cyclosome (APC/C), a ubiquitin ligase that when bound to the activator Cdc20 targets substrates for ubiquitination and subsequent degradation (London and Biggins, 2014b). If chromosomes are not attached to spindle microtubules in metaphase, the spindle checkpoint signals to inhibit APC/C substrate ubiquitination. Spindle checkpoint activation depends on the kinetochore localization of the highly conserved checkpoint proteins Bub1, Bub3, Mad1, and Mad2 (London and Biggins, 2014b). Bub3 localizes to kinetochore protein Knl1/Spc105 and brings Bub1 (London et al., 2012; Shepperd et al., 2012; Yamagishi et al., 2012; Primorac et al., 2013). Recent studies in yeast and *Caenorhabditis elegans* show that Mad1 binds Bub1 and activates Mad2 (London and Biggins, 2014a; Moyle et al., 2014). Ultimately, active Mad2 binds Cdc20 and forms a mitotic checkpoint complex (MCC) with Bub3 and BubR1/Mad3 (Sudakin et al., 2001). The MCC binds the APC/C to block the interaction of Cdc20 with its substrates but still allow Cdc20 autoubiquitination, which promotes Cdc20 turnover during the spindle checkpoint arrest (Pan and Chen, 2004; Braunstein et al., 2007; King et al., 2007; Nilsson et al., 2008; Ge et al., 2009; Herzog et al., 2009; Foe et al., 2011; Mansfeld et al., 2011; Chao et al., 2012).

In addition to their roles in spindle checkpoint signaling, Bub1 and Bub3 facilitate chromosome biorientation, the process in which sister chromatid kinetochores attach to microtubules from opposite spindle poles (van der Horst and Lens, 2014). The Bub1-dependent phosphorylation of histone H2A allows the recruitment of shugoshin to the centromere (Kawashima et al., 2010). Shugoshin (Sgo1 in budding yeast) recruits other proteins needed for kinetochore biorientation, such as the chromosome passenger complex (CPC; van der Horst and Lens, 2014). In budding yeast, the spindle checkpoint proteins are not essential; however, *bub1Δ* and *bub3Δ* cells have an increased rate of chromosome missegregation and grow more slowly than wild-type cells (Hoyt et al., 1991; Li and Murray, 1991; Warren et al., 2002). Whether the growth defect in *bub1Δ* and *bub3Δ* cells is a consequence of the failure to localize the CPC, or caused by the loss of an additional role of Bub1 and Bub3, is unclear.

Here, we find that in the absence of Bub1 or Bub3, the duration of metaphase is longer than in wild-type cells. This result was unexpected because Bub1 and Bub3 are required for spindle checkpoint signaling, which delays cells in metaphase;

Correspondence to Soni Lacefield: sonil@indiana.edu

Abbreviations used in this paper: APC/C, anaphase-promoting complex/cyclosome; CPC, chromosome passenger complex; IP, immunoprecipitation; MCC, mitotic checkpoint complex; SPB, spindle pole body.

The Rockefeller University Press $30.00
J. Cell Biol. Vol. 209 No. 4 519–527
www.jcb.org/cgi/doi/10.1083/jcb.201412036

therefore, the expectation would be that loss of Bub1 or Bub3 would not cause a delay. We find that in *bub3Δ* cells, but not in *bub1Δ* cells, binding of the APC/C and Cdc20 is defective, and the metaphase delay can be rescued by Cdc20 overexpression. Bub3 kinetochore localization is required for the normal timing of anaphase onset and for normal binding of APC/C and Cdc20, suggesting that Bub3 enhances the binding of APC/C and Cdc20 through its interactions with Cdc20 at the kinetochore. Our observations reveal that Bub3 has a previously undiscovered role, independent of the spindle checkpoint, in activating the APC/C in metaphase.

Results and discussion

Anaphase onset is delayed in cells lacking kinetochore-localized Bub1 or Bub3

We used time-lapse microscopy to measure the duration of mitosis in wild-type, *bub1Δ*, and *bub3Δ* cells. The cells expressed Tub1-GFP to monitor spindle assembly and Spc42-mCherry to monitor the separation of spindle pole bodies (SPBs), the yeast equivalent of the centrosome (Fig. 1, A–C). In wild-type cells, the duration from SPB separation to anaphase spindle elongation was 25 ± 1 min (mean ± SEM; Fig. 1, A and D). The duration increased to 44 ± 5 min in *bub1Δ* cells and 42 ± 3 min in *bub3Δ* cells, a statistically significant difference from wild-type cells ($P < 0.0001$, Mann–Whitney test; Fig. 1 D). The *bub1Δ* and *bub3Δ* cells also showed more cell-to-cell variation in cell cycle length (Fig. S1).

Bub1 and Bub3 have known functions at the kinetochore. However, in *Drosophila melanogaster* and human cells certain checkpoint proteins have kinetochore-independent roles in regulating cell cycle progression (Meraldi et al., 2004; Lopes et al., 2005). Therefore, we tested whether Bub1 and Bub3 kinetochore localization is required for normal mitotic progression. We performed time-lapse microscopy on *spc105-6A* and $bub3^{R127A/R239A}$, two mutants that disrupt the interaction between Bub3 and kinetochore protein Spc105, preventing Bub3 kinetochore localization (London et al., 2012; Primorac et al., 2013). Bub3 does not require Bub1 for kinetochore localization, but Bub1 does require Bub3; therefore, *spc105-6A* and $bub3^{R127A/R239A}$ mutants also fail to recruit Bub1 to the kinetochore (Gillett et al., 2004; Primorac et al., 2013). The duration from SPB separation to anaphase onset was delayed in both mutants when compared with wild type, at 43 ± 4 min in *spc105-6A* and 42 ± 4 min in $bub3^{R127A/R239A}$ cells (Fig. 1 D). These results suggest that Bub1 and Bub3 kinetochore localization is required for normal mitotic progression.

At the kinetochore, Bub1 and Bub3 have known roles in signaling the spindle checkpoint and in recruiting Sgo1 (Biggins, 2013). Because Mad2 and Mad3 are required for checkpoint signaling (Li and Murray, 1991), we tested their role in mitotic progression. The *mad2Δ* and *mad3Δ* cells progress through mitosis with similar timing as wild-type cells (Fig. 1 D). To test the role of Sgo1 recruitment in the normal timing of anaphase onset, we analyzed a mutant version of Bub1 with the kinase domain deleted, Bub1-*ΔK*. The kinase activity of Bub1 is not needed for spindle checkpoint signaling but is needed for Sgo1 localization (Warren et al., 2002; Fernius and Hardwick, 2007; Kawashima et al., 2010). Bub1-*ΔK* localizes to the kinetochore but does not phosphorylate histone H2A for Sgo1 localization (Fernius and Hardwick, 2007). We find that *bub1-ΔK* cells have a delay in anaphase onset (Fig. 1 D). Furthermore, *sgo1Δ* cells also have a delay in anaphase onset (Fig. 1 D). The results indicate that Bub1 kinase activity and Sgo1 localization are also required for the normal timing of anaphase onset.

The delay in cell cycle progression in *bub3Δ* cells is not caused by activation of the G2/M, DNA damage, or spindle position checkpoints

The increased duration of mitosis in *bub1Δ* and *bub3Δ* cells could be a result of the activation of a checkpoint, such as the G2/M, DNA damage, and spindle position checkpoints. We deleted genes required for each checkpoint in combination with *bub3Δ* to determine whether the mutation rescues the delay in anaphase onset. In *bub3Δ chk1Δ*, *bub3Δ swe1Δ*, and *bub3Δ bub2Δ* cells, anaphase onset was delayed in comparison to wild-type cells, similar to the delay in *bub3Δ* cells (Fig. 1 E). The *bub3Δ mad2Δ* cells also have a delay in anaphase onset. The results suggest that the loss of Bub3 does not delay anaphase onset by activating the G2/M, DNA damage, spindle position, or spindle checkpoints.

Metaphase is delayed in cells lacking Bub1 or Bub3

The budding yeast spindle forms at the end of S phase (Biggins, 2013). Therefore, a cell cycle delay from SPB separation to anaphase onset could be a result of G2 or metaphase delay. To determine whether *bub1Δ* and *bub3Δ* cells were delayed in metaphase, we monitored cells released from a metaphase arrest and measured the duration to anaphase onset. Cells are reversibly arrested in metaphase by placing the APC/C activator Cdc20 under the control of the methionine-repressible *MET3* promoter ($P_{MET}CDC20$; Uhlmann et al., 2000). The $P_{MET}CDC20$, *bub1Δ* $P_{MET}CDC20$, *bub3Δ* $P_{MET}CDC20$, and *bub1-ΔK* $P_{MET}CDC20$ cells arrested in metaphase in medium containing methionine were released from the arrest by washing out the medium and adding medium lacking methionine. The $P_{MET}CDC20$ cells enter anaphase in 22 ± 1 min. The *bub3Δ* $P_{MET3}CDC20$, *bub1Δ* $P_{MET3}CDC20$, and *bub1-ΔK* $P_{MET}CDC20$ cells have a statistically significant delay in anaphase onset compared with wild-type cells and enter anaphase after 36 ± 4, 33 ± 3, and 31 ± 3 min, respectively (Fig. 1 F).

Furthermore, we measured the duration that kinetochores were bioriented, or attached to opposite spindle poles in *bub1Δ* and *bub3Δ* cells. To assess biorientation, we monitored the separation of a tagged kinetochore protein Mtw1-GFP. Bioriented sister chromatid kinetochores are pulled ∼0.8 µm apart (Joglekar et al., 2008). In wild-type cells, kinetochores are bioriented for 23 ± 1 min. In *bub1Δ* and *bub3Δ* cells, the duration that kinetochores are bioriented is increased to 42 ± 3 min and 44 ± 3 min, respectively (Fig. 1 G). The duration is also increased in *bub1-ΔK*, *sgo1Δ*, and $bub3^{R127A/R239A}$ cells. In summary,

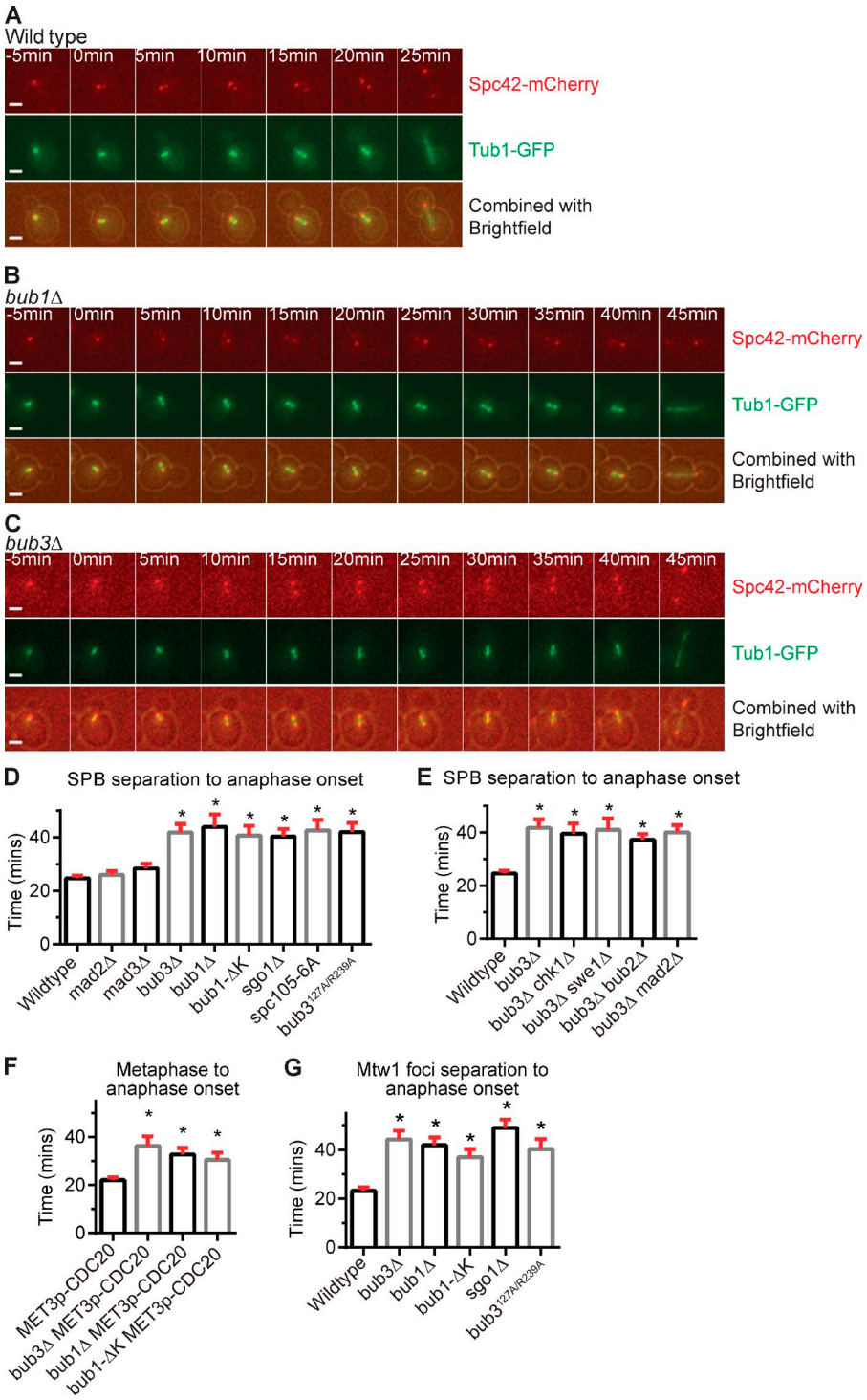

Figure 1. **Anaphase onset is delayed in the absence of kinetochore-localized Bub1 or Bub3.** (A–C) Time-lapse images of wild-type, *bub1Δ*, and *bub3Δ* cells with Spc42-mCherry and Tub1-GFP. Bars, 2 µm. (D–G) Plots of the mean time (in minutes) for each genotype. At least 50 cells were counted per genotype. Error bars are the SEM. Asterisks indicate a statistically significant difference compared with wild-type cells (*, $P < 0.0001$, Mann–Whitney test). (D and E) Time from SPB separation to anaphase onset. (F) Time from metaphase to anaphase onset in strains with *CDC20* under the repressible *MET3* promoter. (G) Time from Mtw1-GFP foci separation to anaphase onset.

the results suggest that *bub1Δ*, *bub3Δ*, *bub1-ΔK*, *sgo1Δ*, and *bub3*$^{R127A/R239A}$ cells are delayed in metaphase with bioriented sister chromatid kinetochores.

APC/C substrates accumulate in *bub1Δ* and *bub3Δ* cells

We monitored the timing of APC/C substrate degradation. Cells were arrested in G1 with α factor and released from the arrest, and then the protein was isolated every 20 min for one cell cycle, adding α-factor back to the cells to ensure that they do not go through another cell cycle. The normal timing of degradation of three APC/C substrates Pds1-9Myc, Clb2, and Clb5 was delayed in *bub1Δ* and *bub3Δ* cells compared with wild-type cells (Fig. 2, A–H). In *bub1Δ* and *bub3Δ* cells, the APC/C substrates were present at times when they should be degraded, such as in G1 (0, 120, and 140 min), as scored by the presence of unbudded cells without a spindle and with Sic1-3HA, a Cdk inhibitor that is present in G1 (Fig. 2, A–H). These results demonstrate that APC/C substrates are not degraded with normal timing in *bub1Δ* and *bub3Δ* cells.

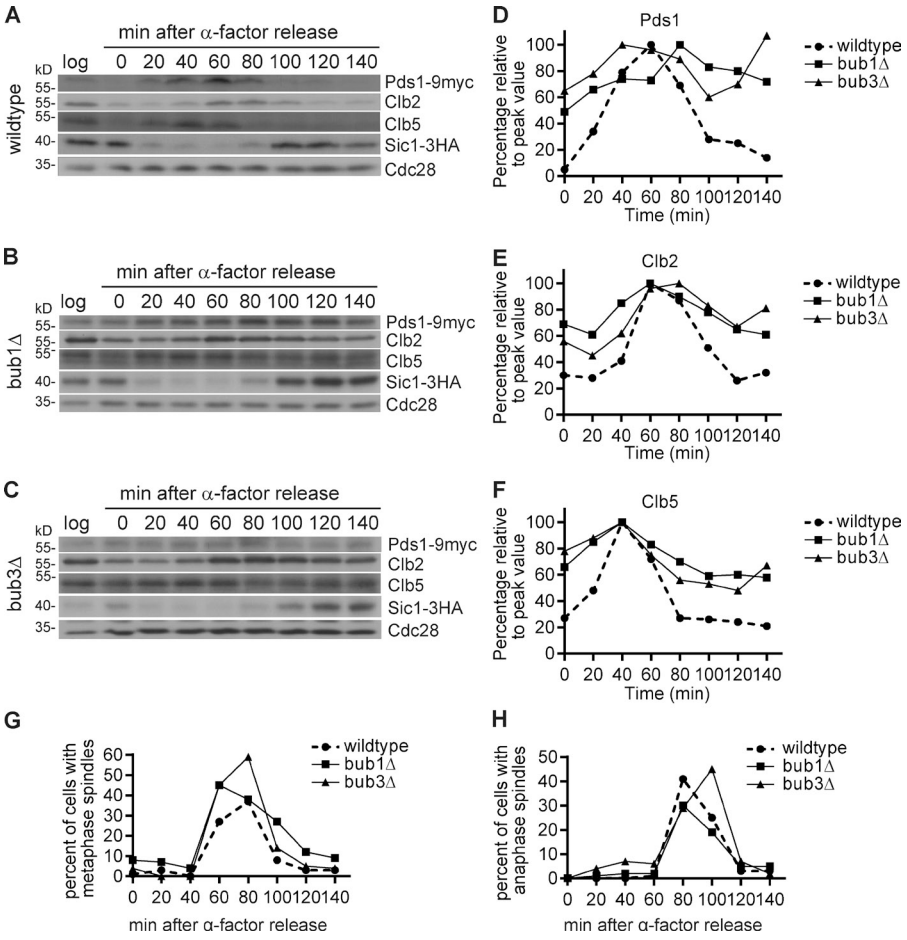

Figure 2. **APC/C-Cdc20 substrate degradation is delayed in *bub1Δ* and *bub3Δ* cells.** (A–C) The degradation of APC/C-Cdc20 substrates Pds1, Clb2, and Clb5 in wild-type (A), *bub1Δ* (B), and *bub3Δ* (C) cells from 20-min time points taken after release from α-factor. Sic1 indicates the cell cycle progression, and Cdc28 served as a loading control. Log represents cells growing at logarithmic phase. (D–F) Protein quantification of Pds1 (D), Clb2 (E), and Clb5 (F), divided by the Cdc28 loading control and then normalized to their peak values. (G and H) Cell cycle progression by percentage of cells with metaphase (G) or anaphase (H) spindles.

The metaphase delay in *bub3Δ* cells is not caused by the accumulation of aneuploid cells

Although most aneuploid cells are delayed in G1, an additional copy of certain chromosomes can result in cells delayed in metaphase (Torres et al., 2007; Thorburn et al., 2013). Because *bub1Δ* and *bub3Δ* cells have a higher rate of chromosome missegregation than wild-type cells (Warren et al., 2002), we were concerned that the aneuploid cells could increase the mean metaphase length of the population. To ensure that we excluded the aneuploid cells from our analysis of metaphase duration in *bub3Δ* cells, we analyzed newly germinated *bub3Δ* spores from a BUB3/*bub3::LEU2* heterozygote (Fig. 3 A). By observing the first several divisions of a newly germinated cell, we could determine whether a chromosome missegregation event occurred; the resulting cell missing a chromosome would die, whereas the cell with an extra chromosome would divide slowly. During our analysis, 100% of the spores from the BUB3/*bub3::LEU2* heterozygote germinated, suggesting that meiotic chromosome segregation was normal (missegregation of a chromosome in meiosis leads to dead spores). After germination and the initial cell division, only 3% of the *bub3::LEU2* spores conferred dead or arrested cells in the first four divisions. To ensure that we did not include aneuploid cells in our analysis, we did not analyze the lineages with dead or arrested cells.

We dissected the tetrads from the BUB3/*bub3::LEU2* heterozygote on an agar pad containing medium lacking leucine such that only the *bub3::LEU2* spores will germinate (Fig. 3 A). We performed the same analysis with wild-type cells with an integrated vector containing *LEU2*. In both wild-type and *bub3Δ* cells, the first cell cycle upon germination was slower at all stages than the next cell cycles, so we averaged the second, third, and fourth cell cycles, counting ≥50 cell divisions for each genotype. Anaphase onset was indeed significantly delayed in *bub3Δ* cells at 33 ± 1 min compared with 24 ± 1 min in wild-type cells ($P < 0.0001$, Mann–Whitney test; Fig. 3 B). Similar analysis from the spores of the Bub3/*bub3*$^{R127A/R239A}$ heterozygote showed that the *bub3*$^{R127A/R239A}$ cells also have a delay in anaphase onset similar to *bub3Δ* cells (Fig. 3 B). The mean time of metaphase in the newly germinated *bub3Δ* and *bub3*$^{R127A/R239A}$ cells is somewhat decreased when compared with the corresponding log phase–grown cultures, and there is less cell-to-cell variation, suggesting that some cells in the log phase cultures were likely aneuploid (Figs. 3 B and S2). Nonetheless, the results demonstrate that *bub3Δ* and *bub3*$^{R127A/R239A}$ cells have a metaphase delay that is not a consequence of aneuploidy. Unfortunately, we could not perform the same analysis for *bub1Δ* because very few spores of the *BUB1*/*bub1Δ* heterozygote germinated, suggesting that two copies of BUB1 are required for

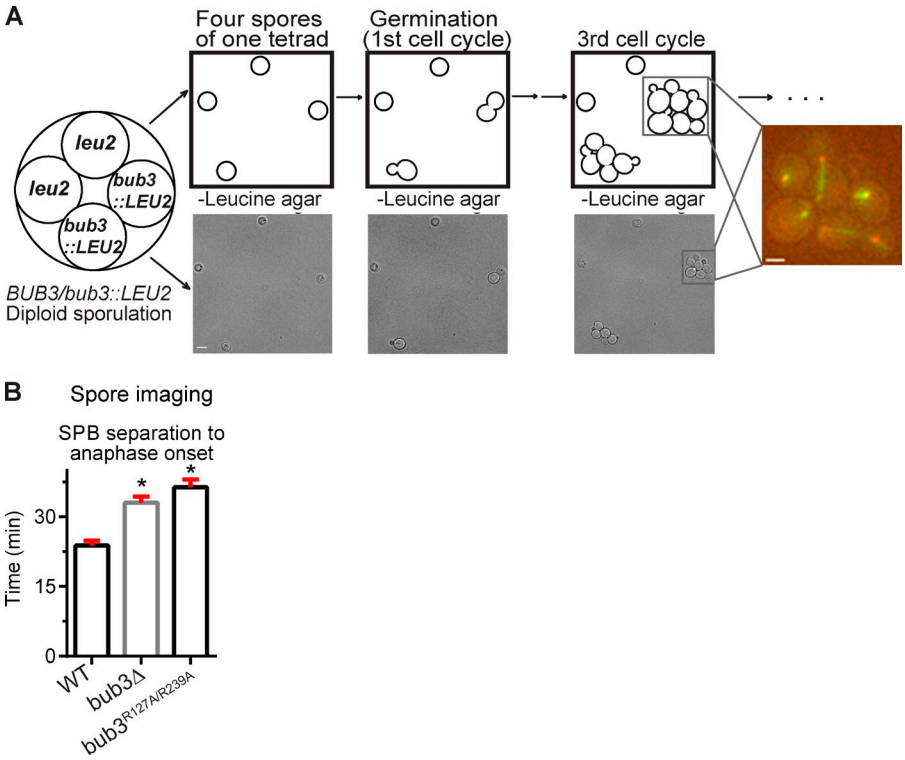

Figure 3. **Newly germinated euploid *bub3Δ* and *bub3*$^{R127A/R239A}$ cells are delayed in anaphase onset.** (A) Schematic of the spore imaging procedure. The first through third cell cycles are represented in the drawing and brightfield images. A fluorescent image of the third cell cycle focuses on one spore germination. Bars: (left) 5 µm; (right) 2 µm. (B) Plot of the mean time from SPB separation to anaphase onset analyzed from spore imaging time-lapse microscopy. Asterisks indicate a statistically significant difference compared with wild type (*, $P < 0.0001$, Mann–Whitney test). Error bars are the SEM. At least 50 cell divisions were counted per genotype. WT, wild type.

normal chromosome segregation in meiosis. We conclude that kinetochore-localized Bub3 promotes the normal duration of metaphase.

The binding of Cdc20 to the APC/C is impaired in the absence of Bub3

Because the metaphase activation of the APC/C requires the association of APC/C with Cdc20 (Visintin et al., 1997; Lorca et al., 1998), we used coimmunoprecipitation (co-IP) to examine the interaction between the APC/C and Cdc20 in wild-type, *bub1Δ*, *bub3Δ*, *sgo1Δ*, and *bub1-ΔK* cells transitioning into anaphase. Cells were arrested in G1 with α-factor, released from the arrest, and then collected at the transition into anaphase. The cells express *CDC23-3HA*, a tagged component of the APC/C, allowing the IP of the APC/C with anti-HA antibodies. Antibodies against Cdc20 detected the amount of Cdc20 in the IP. In the no tag control, Cdc23 and Cdc20 were not detected in the IP, showing that the IP was specific to tagged Cdc23 (Fig. 4 A).

Surprisingly, there was a severe reduction of Cdc20 associated with the APC/C in *bub3Δ* cells compared with wild-type cells (Fig. 4, A and B). Cdc20 levels are not reduced in the input, suggesting that the diminished level of Cdc20 coimmunoprecipitated in *bub3Δ* cells cannot be explained by reduced Cdc20 protein levels (Fig. 4, A and B). Furthermore, similar levels of Cdc23 were immunoprecipitated from each strain (Fig. 4 C). There was a 93% reduction in the ratio of Cdc20 in the IP to Cdc20 in the input ($Cdc20^{IP}/Cdc20^{Input}$) in *bub3Δ* compared with wild type (Fig. 4 B). In contrast to *bub3Δ* cells, the *bub1Δ*, *sgo1Δ*, and *bub1-ΔK* cells do not have reduced levels of Cdc20 bound to APC/C component Cdc23 (Fig. 4, A and B). These results suggest that the binding of APC/C and Cdc20 is impaired in the absence of Bub3 but not Bub1 or Sgo1.

We also assessed whether kinetochore localization of Bub3 was needed for normal binding of the APC/C with Cdc20. In the *bub3*$^{R127A/R239A}$ mutant that does not localize to the kinetochore, the amount of Cdc20 immunoprecipitated with APC/C component Cdc23 is also severely reduced when compared with wild type (Fig. 4, A and B). These results suggest that kinetochore-localized Bub3 is required for the normal binding of the APC/C and Cdc20.

The overexpression of Cdc20 rescues the metaphase delay of bub3Δ cells but not *bub1Δ*, *bub1-ΔK*, or *sgo1Δ* cells

Considering that APC/C and Cdc20 binding is impaired in *bub3Δ* cells, we tested whether increasing Cdc20 levels could suppress the metaphase delay. We overexpressed *CDC20* in wild-type, *bub3Δ*, *bub1Δ*, *bub1-ΔK*, and *sgo1Δ* cells and measured the duration from SPB separation to anaphase onset. Cells with an integrated vector with *CDC20* under the galactose-inducible *GAL1* promoter ($P_{GAL}CDC20$) were grown in galactose medium to overexpress *CDC20*. Cells grow slower in galactose medium than glucose medium, so we compared cells with $P_{GAL}CDC20$ to cells with an integrated empty vector, both growing in galactose medium. In wild-type cells, the duration from SPB separation to anaphase onset is 37 ± 2 min in cells overexpressing *CDC20*, which is similar to the 39 ± 2 min in cells not overexpressing *CDC20* (Fig. 5 A). In contrast, the duration from SPB separation to anaphase onset is shorter in *bub3Δ* cells overexpressing *CDC20* at 41 ± 2 min compared with *bub3Δ* cells not overexpressing *CDC20* at 56 ± 3 min (Fig. 5 A). In the *bub3Δ* cells overexpressing *CDC20*, there was an increase in the number of dead cells when compared with the *bub3Δ* cells not overexpressing *CDC20*, suggesting that the metaphase delay

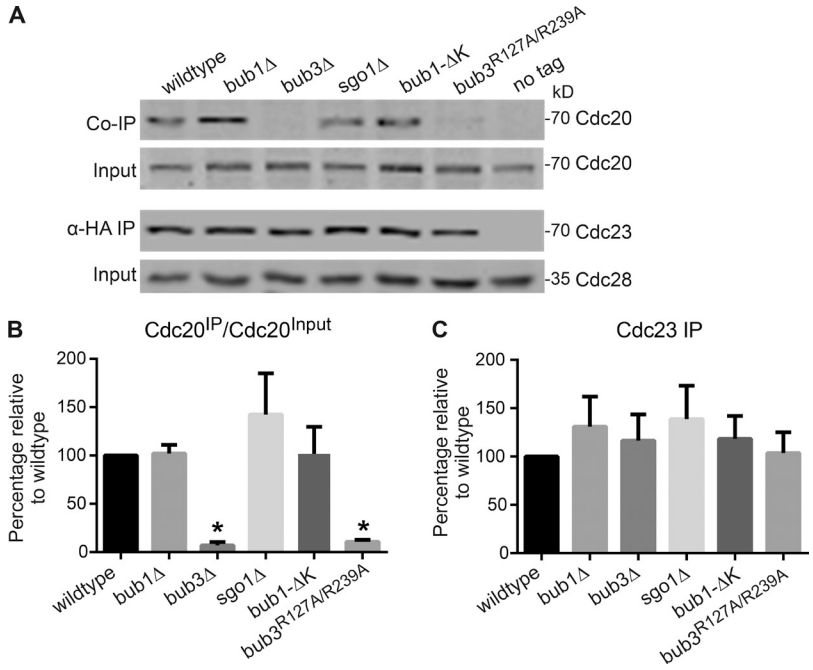

Figure 4. **APC/C-Cdc20 binding is impaired in *bub3Δ* and *bub3*$^{R127A/R239A}$ cells but not in *bub1Δ*, *sgo1Δ*, or *bub1-ΔK* cells.** (A) Co-IP and input Western blot showing APC/C component Cdc23-3HA and Cdc20 in cells at the metaphase to anaphase transition. Cdc28 serves as a loading control. (B and C) Plots of the mean percentage of Cdc20 bound to Cdc23 (B) and levels of Cdc23 pulled down in the IP (C) from three independent experiments. Values were normalized to wild type. Error bars are the SD. Asterisks indicate a statistically significant difference compared with wild type (*, $P < 0.001$, unpaired *t* test with Welch's correction).

may allow increased cell survival. We conclude that overexpression of Cdc20 rescues the metaphase delay in *bub3Δ* cells.

In contrast to *bub3Δ* cells, the duration of metaphase is not shortened in *bub1Δ*, *bub1-ΔK*, or *sgo1Δ* cells overexpressing *CDC20* when compared with the respective genotype that does not overexpress *CDC20* (Fig. 5 A). These results and the results from the co-IP experiments suggest that although *bub1Δ* and *bub3Δ* cells both have a metaphase delay, the delay may be caused by different mechanisms. In the absence of Bub1, a failure to localize Sgo1 and the CPC to the kinetochore may lead to a metaphase delay. In support of this model, a previous study showed that the growth defect of *sgo1Δ* cells can be rescued by a mutant of Sli15, *sli15(ΔNT)*, which bypasses the requirement for CPC clustering between sister kinetochores (Campbell and Desai, 2013). However, in the absence of Bub3, the metaphase delay can be rescued by *CDC20* overexpression and is therefore likely caused by the impaired interaction between the APC/C and Cdc20.

Bub3 and Cdc20 colocalize to the kinetochore

Because Bub3 kinetochore localization is required for the proper timing of anaphase onset and for full APC/C-Cdc20 binding, we examined the localization of Bub3 and Cdc20 at the kinetochore. Although Cdc20 localizes to kinetochores in many organisms, the localization has not been demonstrated in budding yeast (London and Biggins, 2014b). In intact budding yeast cells, kinetochores are clustered near the SPB, and individual kinetochores cannot be resolved. To examine individual kinetochores, we used mitotic chromosome spreads from protoplasts of cells expressing kinetochore protein Ndc10-6HA, Bub3-EGFP, and 12Myc-Cdc20. Immunofluorescence was performed with anti-HA, anti-GFP, and anti-Myc antibodies. As an example of a protein known to localize to the kinetochore, we show the colocalization of Bub3 and Ndc10 in mitotic chromosome spreads (Fig. 5 B). We find that Cdc20 and Bub3 colocalize, and Cdc20 and Ndc10 colocalize (Fig. 5, C and D). In contrast to Bub3, Cdc20 does not localize to all kinetochores at a single time point, suggesting that the localization of Cdc20 to a kinetochore may be transient. These results demonstrate that Bub3 colocalizes with Cdc20 at the kinetochore.

Conclusion

This study revealed an unexpected role for Bub3 in activating the APC/C for the normal progression of metaphase. In the absence of Bub3, metaphase is delayed, and binding of APC/C and Cdc20 is impaired. Intriguingly, Bub3 must localize to the kinetochore to prevent the metaphase delay, and Bub3 and Cdc20 colocalize at the kinetochore. Our results suggest a new model for the coordination of the metaphase to anaphase transition with kinetochore-localized Bub3 promoting Cdc20 and APC/C binding.

The role of Bub3 in activating APC/C-Cdc20 seems contradictory to its known role in inhibiting APC/C activity during spindle checkpoint signaling. However, the results are consistent when considering that although substrate ubiquitination is blocked during checkpoint signaling, APC/C-Cdc20 autoubiquitinates (Pan and Chen, 2004; Braunstein et al., 2007; King et al., 2007; Nilsson et al., 2008; Ge et al., 2009; Herzog et al., 2009; Foe et al., 2011; Mansfeld et al., 2011; Chao et al., 2012). In vitro experiments using purified budding yeast checkpoint proteins from cells with an active spindle checkpoint show that Bub3-Mad3 stimulates the binding of APC/C and Cdc20 to promote Cdc20 autoubiquitination (Foster and Morgan, 2012). Our in vivo experiments suggest that Bub3 enhances APC/C and Cdc20 binding for normal metaphase progression, independent of spindle checkpoint signaling. We propose that Bub3 normally promotes APC/C and Cdc20 binding; however, when the spindle checkpoint is active, the association of Bub3 with the MCC blocks the interaction

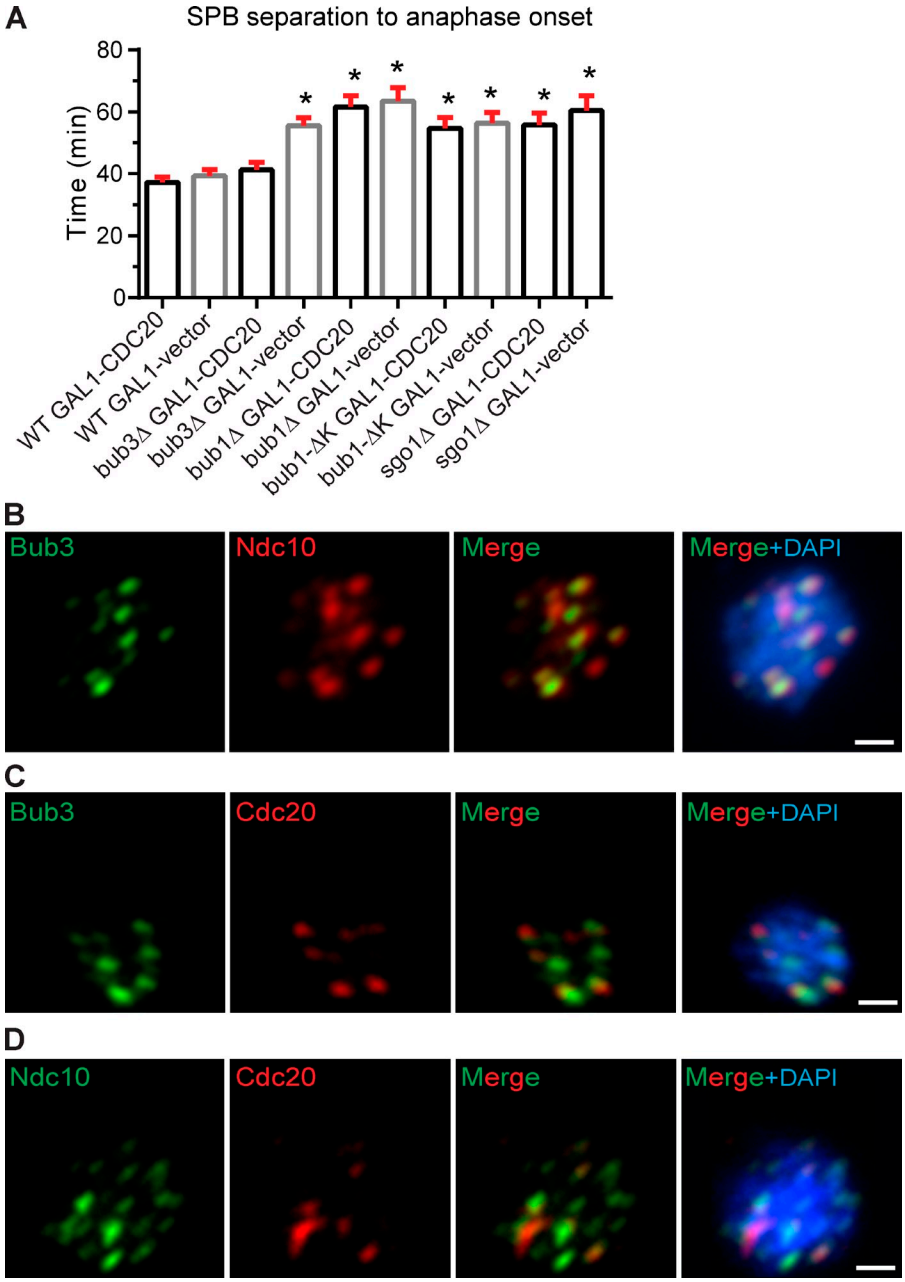

Figure 5. **Anaphase onset timing is restored by *CDC20* overexpression in *bub3Δ* cells but not *bub1Δ*, *sgo1Δ*, *or bub1-ΔK* cells, and Bub3 colocalizes with Cdc20 at the kinetochore.** (A) Plot of the mean time (minutes) from SPB separation to anaphase onset when *CDC20* is overexpressed by an inducible *GAL1* promoter. At least 50 cells were counted per genotype. Error bars are the SEM. Asterisks indicate statistically significant difference compared with wild type (WT) + *GAL1-CDC20* (*, $P < 0.0001$, Mann–Whitney test). (B–D) Immunofluorescence of mitotic chromosome spreads showing Bub3-EGFP and Ndc10-6HA (B), Bub3-EGFP and 12Myc-Cdc20 (C), and Ndc10-6HA and 12Myc-Cdc20 (D). Bars, 1 µm.

of the APC/C with its substrates but still allows Cdc20 autoubiquitination. In summary, Bub3's role in promoting binding of APC/C and Cdc20 is important for normal cell cycle progression and spindle checkpoint signaling.

Materials and methods

Budding yeast strains

All strains are W303 derivatives and are described in Table S1. Deletion and tagged strains were made by PCR amplification and transformation of marked cassettes (Longtine et al., 1998; Janke et al., 2004). For deletions, primers with homology overhangs flanking the open reading frame were used to amplify the cassette. For tagged strains, primers flanking the stop codon of the target genes were used. The P_{GAL}*CDC20* strain was made by PCR amplifying the *CDC20* ORF and cloning it behind the *GAL1,10* promoter in pRS306 and then integrating the plasmid into the URA3 locus. We thank S. Biggins (Fred Hutchinson Cancer Research Center, Seattle, WA), A. Murray (Harvard University, Cambridge, MA), A. Musacchio (Max Planck Institute of Molecular Physiology, Dortmund, Germany), and K. Hardwick (University of Edinburgh, Edinburgh, Scotland, UK) for strains used in this study.

Microscope image acquisition

Cells were imaged with an inverted microscope (Ti-E; Nikon) equipped with a 60× objective (Plan Apochromat NA 1.4 oil), a Lambda 10–3 optical filter changer and SmartShutter, GFP, and mCherry filters, and a charge-coupled device camera (CoolSNAP HQ2; Photometrics) at 25°C. Z stacks of 5–6 sections were acquired in 5–10-min intervals for 12–16 h with a combination of 12.5% neutral density filter and 6.25% neutral density filter and exposure times of 50–900 ms. Z stacks were combined into a single maximum-intensity projection using the maximum-intensity projection function in NIS-Elements software (Nikon). Images were cropped to the same size to show individual cells dividing over time with GFP- and mCherry-tagged proteins.

Time-lapse microscopy

Cells were incubated at 30°C to mid–log phase. Wild-type control cells and mutant cells were put on two side-by-side agar pads containing synthetic

complete medium and imaged together for each video at 25°C. Wild-type cells were checked for the same mean cell cycle duration for each experiment to ensure that conditions were the same in each experiment. Images were acquired in 5-min intervals for 12–16 h with exposure times of 50–900 ms according to fluorescence intensity. In the galactose induction experiments, cells were incubated at 30°C to mid–log phase, and galactose was added to the medium for 3 h before the imaging. Time-lapse microscopy was analyzed for cell cycle duration, and data were graphed in Prism (GraphPad Software). The significance was calculated using the Mann–Whitney test.

Spore imaging

A heterozygous *bub3Δ* strain (LY1897) was constructed by deleting one copy of *BUB3* in a wild-type diploid strain (LY1877). A heterozygous *bub3*$^{R127A/R239A}$ strain (LY2094) was constructed by mating a *bub3*$^{R127A/R239A}$ haploid strain (LY1894) with a wild-type haploid strain (LY1930). Cells were sporulated, and 16–20 tetrads were dissected, arranged on –leucine agarose pads, and mounted on a coverglass surrounded by a humid chamber. Images were acquired in 1-h intervals for 3 h followed by 10-min intervals for 10–12 h to monitor germination and the first four divisions of the spores.

Mitosis time course protein isolation

For the mitosis time course, wild-type (LY1959), *bub3Δ* (LY1990), and *bub1Δ* (LY1988) cells were incubated in YPD (yeast, peptone, dextrose) at 30°C until saturation, diluted 1:20 into 40 ml of fresh YPD, and incubated at 30°C for 3 h. 5 µM α-factor was added for 2 h at 25°C, and cells were checked for >85% shmoos. α-Factor was washed out using 20 ml of fresh YPD three times at room temperature, and cells were resuspended in 40 ml YPD and incubated at 25°C. After 80 min, α-factor was added back to the culture to prevent the cells from going into the next cell cycle. The cell culture (5 ml) was harvested and snap frozen in liquid nitrogen every 20 min after resuspension, and a sample of cells were fixed using 4% paraformaldehyde to check for spindle morphology.

APC/C-Cdc20 co-IP

For the co-IP of Cdc20 and Cdc23-3HA, cells were grown in YPD to saturation overnight at 25°C, diluted into 20 ml of fresh YPD and incubated for 3 h at 25°C. 10 µM α-factor was added for 1.5 h at 25°C. α-Factor was washed out three times using 20 ml YPD, and cells were resuspended in 20 ml YPD at 25°C. Cells were harvested when they were transitioning into anaphase. Cell pellets were divided into two tubes and resuspended in lysis buffer + 1 mM PMSF + protease inhibitor tablet (Roche). Glass beads were added to each tube, and cells were vortexed at 4°C for 7 × 1 min maximum speed, with 1 min on ice in between each vortex. Cell lysates were centrifuged at 13,200 rpm for 5 min. 50–100 µl of cleared lysate was diluted 1:5 using 3×SDS reducing sample buffer and boiled at 95°C for 5 min; 10 µl was loaded for Western blot. 1 µg of mouse α-HA antibody (Roche) was mixed with the remaining cleared lysate and incubated on ice for 20 min. The mixture was then precleared for 2 min at 13,200 rpm, and the supernatant was mixed with 35 µl protein G Dynabeads and incubated on a rotation platform at 4°C for 1 h. The beads were then washed three times with 500 µl Cdc20 bead buffer (200 mM NaCl, 50 mM Tris-Cl, pH 7.4, 50 mM NaF, 5 mM EGTA, 5 mM EDTA, 0.1% NP-40, and 1 mM DTT) and two times with 500 µl low salt kinase buffer (10 mM NaCl, 20 mM Hepes-KOH, pH 7.4, and 5 mM $MgCl_2$), the last wash was transferred to a new microcentrifuge tube, and 20 µl of SDS reducing sample buffer was used to resuspend the beads. The beads were then boiled at 95°C for 5 min, and 10 µl supernatant was loaded for Western blotting. Cdc20 and Cdc23-3HA were blotted on two separate blots because of their close sizes.

Western blotting and quantification

For the Western blots for the mitosis time course and the co-IP, the membrane was cut according to corresponding size of the proteins and incubated with mouse α-myc (1:500; 9E10; Roche), mouse α-HA (1:1,000; 12CA5; Roche), rabbit α-Clb2 (1:1,000; y-180, sc9071; Santa Cruz Biotechnology, Inc.), rabbit α-Cdc28 (1:3,000; PSTAIRE, sc-53; Santa Cruz Biotechnology, Inc.), goat α-Clb5 (1:1,000; yN-19, sc-6704; Santa Cruz Biotechnology, Inc.), and goat α-Cdc20 (1:500; yC-20, sc-6731; Santa Cruz Biotechnology, Inc.). PageRuler Prestained Protein Ladder (Thermo Fisher Scientific) was used, and migration of the bands was indicated in each blot. For the mitotic time course experiments, the secondary antibodies used were donkey anti–rabbit HRP (GE Healthcare), sheep anti–mouse HRP (GE Healthcare), and donkey anti–goat HRP (sc-2033; Santa Cruz Biotechnology, Inc.) at 1:5,000. ECL substrates were added to the washed membrane, and exposure was performed using Classic blue sensitive x-ray film on Konica Minolta X-ray film processor. For the co-IP experiments, the secondary antibodies used were IRDye 800CW donkey anti–goat IgG (C41105-01; LI-COR Biosciences) and IRDye 680RD donkey anti–rabbit IgG (C41009-02; LI-COR Biosciences) at 1:15,000. Blots were processed according to the Li-COR Western blot protocol and imaged using Odyssey CLx (LI-COR Biosciences). All quantifications were processed using Image Studio software (LI-COR Biosciences) and graphed in Prism.

Immunofluorescence

Mitotic cells were fixed with 4% paraformaldehyde for 5 min at room temperature. Cells were washed with PBS, and cell wall was digested with 1 mg/ml zymolyase (Zymo Research) buffered with 1 M sorbitol. Harvested protoplasts were washed with 1 M sorbitol, applied on a slide, and hypotonic solution (0.01 M sorbitol and 0.1% Triton X-100) was added. The slides were washed with PBS and blocked with 5% bovine serum albumin (Sigma-Aldrich) for 1 h at 25°C. For detection of Bub3-EGFP, Ndc10-6HA, and 12Myc-Cdc20, the primary antibodies chicken anti-GFP (1:600; Novus Biologicals), mouse anti-HA (1:500; Santa Cruz Biotechnology, Inc.), and rabbit anti-Myc (1:500; Santa Cruz Biotechnology, Inc.) were applied, respectively, for 15 h at 4°C. Slides were washed twice with PBS, once with PBS containing 0.1% Tween 20, and once with PBS. Secondary antibodies, Alexa Fluor 488–conjugated goat anti–chicken (1:200; Molecular Probes), Alexa Fluor 594–conjugated goat anti–mouse (1:200; Molecular Probes), and Alexa Fluor 594–conjugated goat anti–rabbit (1:200; Molecular Probes) were applied for 1 h at 25°C for imaging. Slides were washed three times with PBS, and DNA was stained with 1 mg/ml DAPI.

Online supplemental material

Fig. S1 shows the variability in the duration of anaphase onset of spindle checkpoint mutants using time-lapse microscopy. Fig. S2 shows the variability in the duration of anaphase onset of newly germinated spores. Table S1 shows strains used in this study. Online supplemental material is available at http://www.jcb.org/cgi/content/full/jcb.201412036/DC1. Additional data are available in the JCB DataViewer at http://dx.doi.org/10.1083/jcb.201412036.dv.

We thank A. Desai and C. Campbell for helpful discussions. We are grateful to S. Biggins, A. Murray, A. Musacchio, and K. Hardwick for strains.

This work was funded in part by Indiana University's Offices of the Vice President and Vice Provost for Research and the Office of the Vice Provost for Research through the Faculty Research Support Program.

The authors declare no competing financial interests.

Submitted: 8 December 2014
Accepted: 16 April 2015

References

Biggins, S. 2013. The composition, functions, and regulation of the budding yeast kinetochore. *Genetics*. 194:817–846. http://dx.doi.org/10.1534/genetics.112.145276

Braunstein, I., S. Miniowitz, Y. Moshe, and A. Hershko. 2007. Inhibitory factors associated with anaphase-promoting complex/cylosome in mitotic checkpoint. *Proc. Natl. Acad. Sci. USA*. 104:4870–4875. http://dx.doi.org/10.1073/pnas.0700523104

Campbell, C.S., and A. Desai. 2013. Tension sensing by Aurora B kinase is independent of survivin-based centromere localization. *Nature*. 497:118–121. http://dx.doi.org/10.1038/nature12057

Chao, W.C., K. Kulkarni, Z. Zhang, E.H. Kong, and D. Barford. 2012. Structure of the mitotic checkpoint complex. *Nature*. 484:208–213. http://dx.doi.org/10.1038/nature10896

Fernius, J., and K.G. Hardwick. 2007. Bub1 kinase targets Sgo1 to ensure efficient chromosome biorientation in budding yeast mitosis. *PLoS Genet.* 3:e213. http://dx.doi.org/10.1371/journal.pgen.0030213

Foe, I.T., S.A. Foster, S.K. Cheung, S.Z. DeLuca, D.O. Morgan, and D.P. Toczyski. 2011. Ubiquitination of Cdc20 by the APC occurs through an intramolecular mechanism. *Curr. Biol.* 21:1870–1877. http://dx.doi.org/10.1016/j.cub.2011.09.051

Foster, S.A., and D.O. Morgan. 2012. The APC/C subunit Mnd2/Apc15 promotes Cdc20 autoubiquitination and spindle assembly checkpoint inactivation. *Mol. Cell*. 47:921–932. http://dx.doi.org/10.1016/j.molcel.2012.07.031

Ge, S., J.R. Skaar, and M. Pagano. 2009. APC/C- and Mad2-mediated degradation of Cdc20 during spindle checkpoint activation. *Cell Cycle*. 8:167–171. http://dx.doi.org/10.4161/cc.8.1.7606

Gillett, E.S., C.W. Espelin, and P.K. Sorger. 2004. Spindle checkpoint proteins and chromosome–microtubule attachment in budding yeast. *J. Cell Biol.* 164:535–546. http://dx.doi.org/10.1083/jcb.200308100

Herzog, F., I. Primorac, P. Dube, P. Lenart, B. Sander, K. Mechtler, H. Stark, and J.M. Peters. 2009. Structure of the anaphase-promoting complex/cyclosome interacting with a mitotic checkpoint complex. *Science*. 323:1477–1481. http://dx.doi.org/10.1126/science.1163300

Hoyt, M.A., L. Totis, and B.T. Roberts. 1991. *S. cerevisiae* genes required for cell cycle arrest in response to loss of microtubule function. *Cell*. 66:507–517. http://dx.doi.org/10.1016/0092-8674(81)90014-3

Janke, C., M.M. Magiera, N. Rathfelder, C. Taxis, S. Reber, H. Maekawa, A. Moreno-Borchart, G. Doenges, E. Schwob, E. Schiebel, and M. Knop. 2004. A versatile toolbox for PCR-based tagging of yeast genes: new fluorescent proteins, more markers and promoter substitution cassettes. *Yeast*. 21:947–962. http://dx.doi.org/10.1002/yea.1142

Joglekar, A.P., E.D. Salmon, and K.S. Bloom. 2008. Counting kinetochore protein numbers in budding yeast using genetically encoded fluorescent proteins. *Methods Cell Biol.* 85:127–151. http://dx.doi.org/10.1016/S0091-679X(08)85007-8

Kawashima, S.A., Y. Yamagishi, T. Honda, K. Ishiguro, and Y. Watanabe. 2010. Phosphorylation of H2A by Bub1 prevents chromosomal instability through localizing shugoshin. *Science*. 327:172–177. http://dx.doi.org/10.1126/science.1180189

King, E.M., S.J. van der Sar, and K.G. Hardwick. 2007. Mad3 KEN boxes mediate both Cdc20 and Mad3 turnover, and are critical for the spindle checkpoint. *PLoS ONE*. 2:e342. http://dx.doi.org/10.1371/journal.pone.0000342

Li, R., and A.W. Murray. 1991. Feedback control of mitosis in budding yeast. *Cell*. 66:519–531. http://dx.doi.org/10.1016/0092-8674(81)90015-5

London, N., and S. Biggins. 2014a. Mad1 kinetochore recruitment by Mps1-mediated phosphorylation of Bub1 signals the spindle checkpoint. *Genes Dev.* 28:140–152. http://dx.doi.org/10.1101/gad.233700.113

London, N., and S. Biggins. 2014b. Signalling dynamics in the spindle checkpoint response. *Nat. Rev. Mol. Cell Biol.* 15:736–748. http://dx.doi.org/10.1038/nrm3888

London, N., S. Ceto, J.A. Ranish, and S. Biggins. 2012. Phosphoregulation of Spc105 by Mps1 and PP1 regulates Bub1 localization to kinetochores. *Curr. Biol.* 22:900–906. http://dx.doi.org/10.1016/j.cub.2012.03.052

Longtine, M.S., A. McKenzie III, D.J. Demarini, N.G. Shah, A. Wach, A. Brachat, P. Philippsen, and J.R. Pringle. 1998. Additional modules for versatile and economical PCR-based gene deletion and modification in *Saccharomyces cerevisiae*. *Yeast*. 14:953–961. http://dx.doi.org/10.1002/(SICI)1097-0061(199807)14:10<953::AID-YEA293>3.0.CO;2-U

Lopes, C.S., P. Sampaio, B. Williams, M. Goldberg, and C.E. Sunkel. 2005. The *Drosophila* Bub3 protein is required for the mitotic checkpoint and for normal accumulation of cyclins during G2 and early stages of mitosis. *J. Cell Sci.* 118:187–198. http://dx.doi.org/10.1242/jcs.01602

Lorca, T., A. Castro, A.M. Martinez, S. Vigneron, N. Morin, S. Sigrist, C. Lehner, M. Dorée, and J.C. Labbé. 1998. Fizzy is required for activation of the APC/cyclosome in *Xenopus* egg extracts. *EMBO J.* 17:3565–3575. http://dx.doi.org/10.1093/emboj/17.13.3565

Mansfeld, J., P. Collin, M.O. Collins, J.S. Choudhary, and J. Pines. 2011. APC15 drives the turnover of MCC-CDC20 to make the spindle assembly checkpoint responsive to kinetochore attachment. *Nat. Cell Biol.* 13:1234–1243. http://dx.doi.org/10.1038/ncb2347

Meraldi, P., V.M. Draviam, and P.K. Sorger. 2004. Timing and checkpoints in the regulation of mitotic progression. *Dev. Cell*. 7:45–60. http://dx.doi.org/10.1016/j.devcel.2004.06.006

Moyle, M.W., T. Kim, N. Hattersley, J. Espeut, D.K. Cheerambathur, K. Oegema, and A. Desai. 2014. A Bub1–Mad1 interaction targets the Mad1–Mad2 complex to unattached kinetochores to initiate the spindle checkpoint. *J. Cell Biol.* 204:647–657. http://dx.doi.org/10.1083/jcb.201311015

Nilsson, J., M. Yekezare, J. Minshull, and J. Pines. 2008. The APC/C maintains the spindle assembly checkpoint by targeting Cdc20 for destruction. *Nat. Cell Biol.* 10:1411–1420. http://dx.doi.org/10.1038/ncb1799

Pan, J., and R.H. Chen. 2004. Spindle checkpoint regulates Cdc20p stability in *Saccharomyces cerevisiae*. *Genes Dev.* 18:1439–1451. http://dx.doi.org/10.1101/gad.1184204

Primorac, I., J.R. Weir, E. Chiroli, F. Gross, I. Hoffmann, S. van Gerwen, A. Ciliberto, and A. Musacchio. 2013. Bub3 reads phosphorylated MELT repeats to promote spindle assembly checkpoint signaling. *eLife*. 2:e01030. http://dx.doi.org/10.7554/eLife.01030

Shepperd, L.A., J.C. Meadows, A.M. Sochaj, T.C. Lancaster, J. Zou, G.J. Buttrick, J. Rappsilber, K.G. Hardwick, and J.B. Millar. 2012. Phosphodependent recruitment of Bub1 and Bub3 to Spc7/KNL1 by Mph1 kinase maintains the spindle checkpoint. *Curr. Biol.* 22:891–899. http://dx.doi.org/10.1016/j.cub.2012.03.051

Sudakin, V., G.K. Chan, and T.J. Yen. 2001. Checkpoint inhibition of the APC/C in HeLa cells is mediated by a complex of BUBR1, BUB3, CDC20, and MAD2. *J. Cell Biol.* 154:925–936. http://dx.doi.org/10.1083/jcb.200102093

Thorburn, R.R., C. Gonzalez, G.A. Brar, S. Christen, T.M. Carlile, N.T. Ingolia, U. Sauer, J.S. Weissman, and A. Amon. 2013. Aneuploid yeast strains exhibit defects in cell growth and passage through START. *Mol. Biol. Cell*. 24:1274–1289. http://dx.doi.org/10.1091/mbc.E12-07-0520

Torres, E.M., T. Sokolsky, C.M. Tucker, L.Y. Chan, M. Boselli, M.J. Dunham, and A. Amon. 2007. Effects of aneuploidy on cellular physiology and cell division in haploid yeast. *Science*. 317:916–924. http://dx.doi.org/10.1126/science.1142210

Uhlmann, F., D. Wernic, M.A. Poupart, E.V. Koonin, and K. Nasmyth. 2000. Cleavage of cohesin by the CD clan protease separin triggers anaphase in yeast. *Cell*. 103:375–386. http://dx.doi.org/10.1016/S0092-8674(00)00130-6

van der Horst, A., and S.M. Lens. 2014. Cell division: control of the chromosomal passenger complex in time and space. *Chromosoma*. 123:25–42. http://dx.doi.org/10.1007/s00412-013-0437-6

Visintin, R., S. Prinz, and A. Amon. 1997. CDC20 and CDH1: a family of substrate-specific activators of APC-dependent proteolysis. *Science*. 278:460–463. http://dx.doi.org/10.1126/science.278.5337.460

Warren, C.D., D.M. Brady, R.C. Johnston, J.S. Hanna, K.G. Hardwick, and F.A. Spencer. 2002. Distinct chromosome segregation roles for spindle checkpoint proteins. *Mol. Biol. Cell*. 13:3029–3041. http://dx.doi.org/10.1091/mbc.E02-04-0203

Yamagishi, Y., C.H. Yang, Y. Tanno, and Y. Watanabe. 2012. MPS1/Mph1 phosphorylates the kinetochore protein KNL1/Spc7 to recruit SAC components. *Nat. Cell Biol.* 14:746–752. http://dx.doi.org/10.1038/ncb2515